Infrared analysis of bone in health and disease

Adele Boskey
Weill Medical College of Cornell University
Program in Musculoskeletal Integrity
Hospital for Special Surgery
Department of Biochemistry
New York, New York 10021
and
Weill Graduate Medical School of
Cornell University
Program in Physiology, Biophysics,
and Systems Biology
New York, New York 10021

Richard Mendelsohn
Rutgers University
Department of Chemistry and Programs in
Applied Physics and Biological Sciences
Newark, New Jersey 07102

Abstract. Infrared spectroscopy, microspectroscopy, and microspectroscopic imaging have been used to probe the composition and physicochemical status of mineral and matrix of bone in normal and diseased tissues using a series of validated parameters that reflect quantitative and qualitative properties. In this review, emphasis is placed on changes in bone's composition and physiochemical status during osteoporosis and the impact of currently used therapeutics on these parameters, although the impact of infrared microscopy in other pathological states is briefly discussed. [DOI: 10.1117/1.1922927]

Keywords: bone; hydroxyapatite; collagen; infrared microspectroscopy; infrared microspectroscopic imaging.

Paper SS04141 received Jul. 23, 2004; revised manuscript received Aug. 19, 2004; accepted for publication Aug. 19, 2004; published online Jun. 15, 2005.

1 Introduction

Bone is a composite tissue that consists of mineral, organic matrix, water, and cells. Bone provides mechanical strength and protection to the body, and maintains mineral ion homeostasis. Always in a dynamic state, bone is deposited by cells known as osteoblasts, and removed by multinucleated cells known as osteoclasts. This formation and resorption process is often referred to as ''remodeling.'' When either of these processes is impaired or excessive, bone no longer has optimal mechanical properties. The best-known example of this imbalance between bone formation and bone resorption occurs in osteoporosis,[1–3] a disease that affects both women and men, and sometimes children,[4] and is characterized by an increase in porosity resulting in an increased risk of fracture. After a first fracture, the risk of sustaining a second fracture is extremely high.[3] Osteoporosis may occur because osteoclasts are too active or because osteoblasts are inactive. The purpose of this review is to describe how infrared spectroscopy is helping us understand the changes in osteoporotic bone before and after therapeutic intervention, and to illustrate how other bone diseases can be studied with infrared (IR).

Infrared analysis was first applied to bone more than half a century ago.[5,6] It was initially used to confirm the x-ray diffraction result that bone mineral was analogous to the naturally occurring geologic mineral, hydroxyapatite (HA) (Fig. 1).[5] As instrumental sophistication increased, IR was used to determine the presence and nature of IR active bone impurities (HPO_4, CO_3), which substitute in HA lattice positions.[6–8] IR and Fourier-transform IR (FTIR) were similarly used to demonstrate changes in HA composition caused by diet,[9–11] space flight,[12] and chronic hypoperfusion.[13] IR spectroscopy was used in 1966 to describe the changes in the crystal size and perfection of the bone apatite particles (% crystallinity).[14] The increases in size and perfection were correlated with the sharpening of the *c*-axis x-ray diffraction peak. It should be noted that based on x-ray diffraction one cannot distinguish absolute increases in crystallite size from formation of a stoichiometrically more perfect lattice structure. The change in x-ray diffraction pattern was initially described as a transition from an amorphous (noncrystalline) calcium phosphate to a poorly crystalline hydroxyapatite,[14] but later was recognized as the maturation of nanoparticles of hydroxyapatite.[15] FTIR spectroscopy has frequently been used to characterize the mineralized matrix formed in cell and organ cultures (e.g., Refs. 16–21), and recently it has been used to demonstrate the properties of the tissue formed on bone-inductive materials.[22–24] IR spectroscopy was also used to identify the presence of bone-like mineral in pathologic (abnormal) mineral deposits.[25–28]

The more recent instrumental advance in which a FTIR spectrometer is coupled with an optical microscope revolutionized the FTIR study of bone by enabling spectra to be acquired at anatomically discrete sites. This was extremely important because bone is a heterogeneous tissue (Fig. 2) and spatial variation had previously been lost due to the need to homogenize the bone before analysis. With FTIR microspectroscopy, spectra could be obtained at sites along an osteon (Fig. 3)[29] or during the process of new bone deposition.[30]

Addition of a focal plane array detector to the infrared microscope was another major advance in the IR analysis of bone as it allowed about a thousand fold increase in the speed of data acquisition. With the concomitant improvements in computer processing capabilities, hyperspectral images consisting of a complete mid IR spectrum at each *x*, *y* location in a thin section (see Fig. 3) can be readily acquired. In these images each pixel corresponds to a point in the *x*-*y* plane of the sample, with the *z* axis corresponding to the magnitude of the desired IR parameter (univariate or multivariate) at that site. Fourier-transform infrared microspectroscopic imaging was rapidly applied to the description of anatomic changes in bone properties,[31] analyses of mineralization in cell cultures,[32]

Address all correspondence to Adele Boskey, Musculoskeletal Integrity Program, Hospital for Special Surgery, 535 E 70th Street, New York, New York 10021.

1083-3668/2005/$22.00 © 2005 SPIE

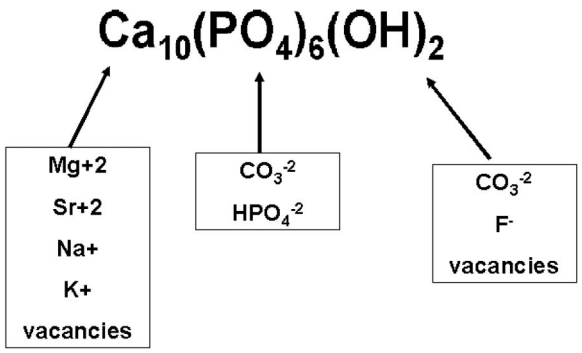

Fig. 1 Structural formula for the hydroxyapatite lattice showing substituents that might be found in each lattice site.

and characterization of bone formation on implant materials.[33,34] It has been most extensively applied to evaluation of diseased bone, which will be the main subject of this review.

There are limitations to IR imaging and microspectroscopy that should be noted. As discussed later, thin (2–6 μm) sections are required, and the samples cannot be examined in a hydrated form because of water interference with the spectra. While reflectance spectra can be used to examine thick specimens, there are reflectance artifacts that still remain to be overcome before surface reflectance can be applied. Perhaps the greatest limitation is that to do an IR analysis of bone a biopsy is required, thus this is an invasive technique.

A typical spectrum of ground bone is shown in Fig. 4. Only the frequencies relevant to the analyses of bone composition are shown. There are phosphate vibrations, carbonate vibrations, representing the extent and nature of carbonate substitution in the HA lattice, and strong protein peaks (Amide I, Amide II, Amide A). The latter arise from peptide bond C=O stretch, mixed N–H in plane bending and C=O stretch and N–H stretching, respectively. These protein bands arise mainly from collagen which accounts for almost 95% of the organic matrix. The other 5% of the matrix contains noncollagenous extracellular matrix proteins whose functions are reviewed elsewhere,[35] lipids, and cell components.

A quantitative assessment of the mineral content of the bone being analyzed can be made by calculating the ratio of the integrated phosphate $\upsilon 1$, $\upsilon 3$, and amide I peaks. Mixtures of collagen and synthetic HA have been analyzed both by gravimetric and FTIR analyses and shown to be linearly related validating this ratio.[36] Carbonate to phosphate ratios can similarly be calculated from their respective integrated areas, and these ratios can be used to follow the incorporation of carbonate into the bone mineral.[37] Deconvolution of the carbonate bands can be used to determine whether the carbonate is substituting for phosphate or hydroxide.[6,7] The validation of the carbonate: phosphate ratio was done by chemical measurements of carbonate content.[38,39]

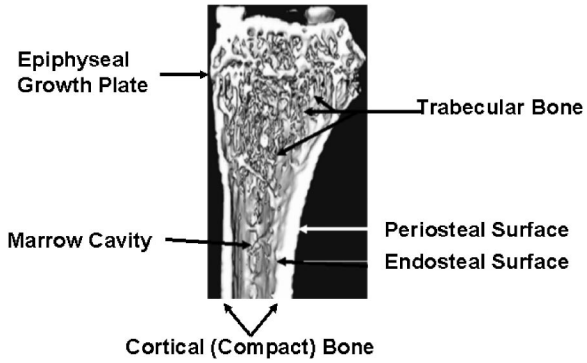

Fig. 2 Three-dimensional view of half a mouse femur based on micro-computerized tomography. Bone components discussed in the text are illustrated, including cortical bone with its periosteal and endosteal surfaces, the growth plate, and individual trabeculae.

2 Methods for FTIR Analyses of Bone

Bone, by its very nature, is a hard material, and hence, it is extremely difficult to prepare the thin sections required for microscopic examination in the visible spectral region. Sections thicker than 5–6 μm do not transmit sufficient light, hence, IR analysis of bone routinely requires samples 2–5 μm in thickness. To circumvent the problem of obtaining thin sections, pathologists routinely embed bone in a resin that is harder than the bone itself. This embedded bone mixture can then be sectioned on a microtome with a diamond or tungsten knife. While this facilitates specimen preparation, the process induces complications in the IR analysis of bone. The embedding materials all have IR active modes, and thus spectral subtraction must be used to remove these contributions.[40] While spectral subtraction of embedding media is fairly straight forward for single spectra [there is a unique band for poly(methylmethacrylate) (PMMA), the most common embedding material, at 1729 cm^{-1}] it is more of a challenge when subtracting PMMA from hyperspectral cubes containing thousands of spectra, and specialized algorithms have been developed for this purpose. Specifically, using ISYS software (Spectral Dimensions, Olney, MD), spectra in the region of interest are truncated, baseline corrected, and ''normalized'' to a pixel containing only PMMA, making each PMMA intensity in the cube equal to 1.0. The normalized PMMA spectrum is then subtracted from each of the normalized spectra, creating spectra at each pixel that are either 0 if the region contained only PMMA, or no evidence of the PMMA band.

The bone sites utilized for data collection are dependent on the question being asked. For example, when temporal changes in bone development are of interest, scans going from the outer bone forming surface (periosteum) to the inner bone resorbing surface (endosteum) are most useful (Fig. 2). If comparisons are made between a diseased and a healthy bone, different areas (cortex, trabeculae) may be examined.

Parameters that are measured in addition to the earlier-mentioned mineral: matrix ratio and carbonate: phosphate ratio are crystallinity,[38,41] collagen maturity,[42] and acid phosphate content.[43] Several of these parameters, as described later, have been validated by independent methods. Mineral to matrix ratio is correlated to the ash content when synthetic mixtures of hydroxyapatite and collagen are analyzed by both methods (Fig. 5).[36] As reviewed elsewhere,[2,36] increasing mineralization leads to stronger bones, although when there is excessive mineralization bones can become brittle.

The crystallinity parameter (1030/1020 peak area ratio) was validated by comparison with x-ray diffraction analysis of HA particle size.[38] Investigation of the collagen maturity

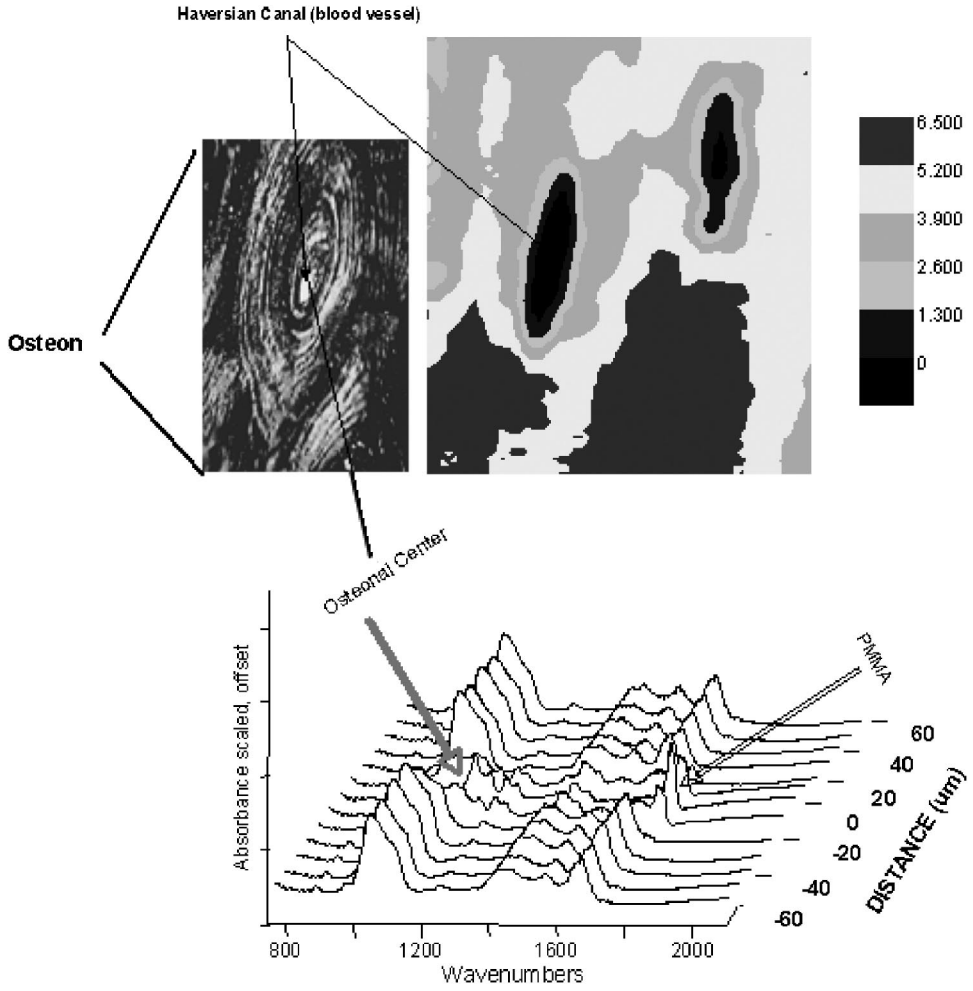

Fig. 3 Osteonal bone. A FTIR image illustrating the variation in mineral: matrix ratio along with a photomicrograph showing the concentric rings around the blood vessel in the center of the osteon, and individual spectra taken 20 μm apart along the osteon.

parameter which is related to the presence of stable collagen crosslinks, is currently in progress using type I collagen peptides whose composition was determined by HPLC. Whereas with FTIR microscopic data, the mineral parameters can be calculated by resolving the peaks in the complex ν_1, ν_3 contour using curve-fitting, two-dimensional-IR, spectral deconvolution or other methods),[44] for FTIR images, the large number of spectra which would have to be analyzed precludes the use of these algorithms, since each spectrum has to be individually examined. The need to analyze thousands of spectra in an image led to the use of intensities at particular frequency positions, rather than peak areas to represent the concentration of a particular component. While these intensities are linearly correlated with the same data obtained by curve-fitting based

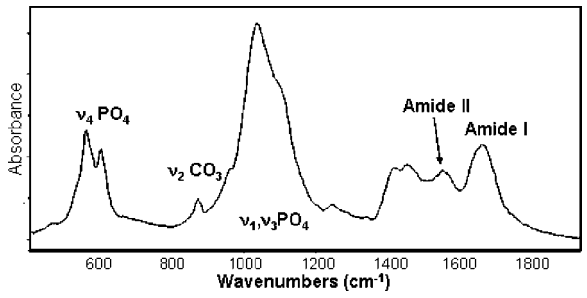

Fig. 4 FTIR spectrum of ground adult mouse bone showing frequencies of interest.

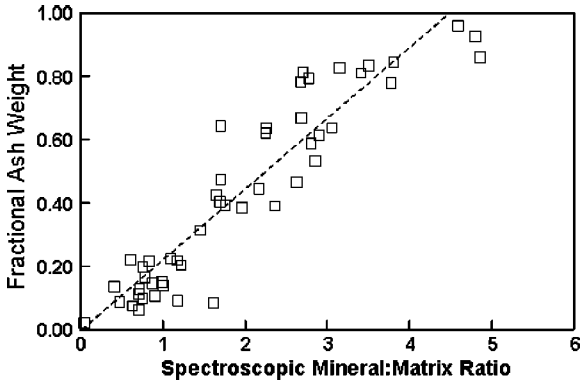

Fig. 5 Development of spectra structure correlation. Spectrally determined mineral matrix ratio correlates with conventionally determined ash weight.

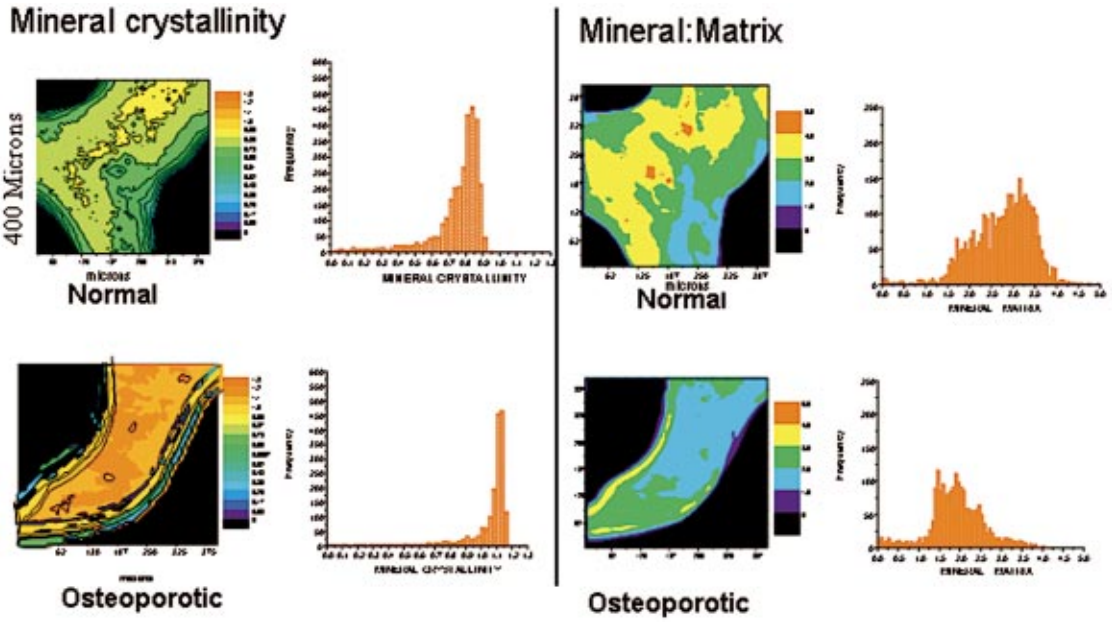

Fig. 6 Image of trabecular bone in normal and osteoporotic females. Right figure shows mineral: matrix ratio and left figure shows crystallinity.

on a pixel by pixel comparison,[45] the range of intensity values is narrower than the range of peak area values, making the intensity ratio less sensitive because of a loss of dynamic range.

The composite picture of each of these parameters, whether obtained from imaging or point-by-point microscopic data, gives an image of the composition, crystallinity, and amount of bone mineral. We believe that one or more of these IR parameters are major predictors of ''bone quality'' or the tendency of bone to fracture. Other factors influencing bone quality are bone geometry, bone microarchitecture (especially connectivity), the presence of microcracks, and the density of the bones. Bone quality is altered with age, as mineral content increases, crystallinity reach maximal values, and collagen matures.[46] Our laboratory is trying to correlate spectroscopic changes in bone IR parameters with changes in mechanical properties, either tested in the same sample or in adjacent tissue. There are limited data indicating that crystal size matters and that a broad distribution of mineral: matrix and crystallinity values is found in healthier bones.[46] There is also a strong indication that crystal size is related to mechanical strength, as shown in a study by Turner in which the crystal thickness was inversely related to strength in fluoride treated animals.[47] Since HA crystal thickness decreases with age as crystal length increases, this is in accord with our preliminary data that mechanical strength is greater when average crystallinity is greater. Recently Raman spectroscopy has also shown an inverse correlation between crystallinity and elastic deformation in a rat aging model.[48]

3 Bone Quality

The quality of bone refers to its optimal ability to perform its functions, as described in terms of bone strength. Bone strength in turn is determined in part by both geometric and material properties,[49] bone mineral density,[50] bone connectivity (whether trabecular bone struts are connected),[51] and genetics.[52] We have proposed the features of bone characterized by IR parameters also contribute to bone strength, and are demonstrating that they show variation in both health and disease.

3.1 *Age and Sex Dependent Changes in Normal Bone*

Infrared microspectroscopic and imaging studies have demonstrated that there are spatial changes in each of the bone spectrum-derived properties with tissue age (Fig. 3), and average changes with animal age.[46] There are also male and female differences which may reflect the differences in rates of growth in different sexes. The tissue- and animal-age dependent changes also vary with the type of bone being examined, but in general until the individual reaches peak bone age there is an increase in mineral: matrix ratio, carbonate: phosphate ratio, crystallinity, and collagen maturity.[46,53] Once adulthood is reached, the bone parameters are relatively invariant, unless there is evidence of bone disease.

3.2 *Osteoporotic versus Normal Bone*

The first IR analyses of bones from osteoporotic patients[54,55] as reviewed elsewhere[56] were inconclusive, because tissues had been homogenized and some contained sites of recent fractures. IR microspectroscopy and imaging facilitated the description of the changes occurring in bones of humans and animals with osteoporosis.

Using biopsies from patients who had sustained osteoporotic fractures, but were at a distance from the fracture site, our studies consistently showed a decrease in mineral content, an increase in crystallinity, and an increase in collagen maturity in both the trabecular and cortical bones of the patients as contrasted with age-matched controls.[57,58] More significantly the age-dependent temporal changes in these parameters were not detected in the untreated osteoporotic patients. Figure 6 compares the mineral content and crystallinity

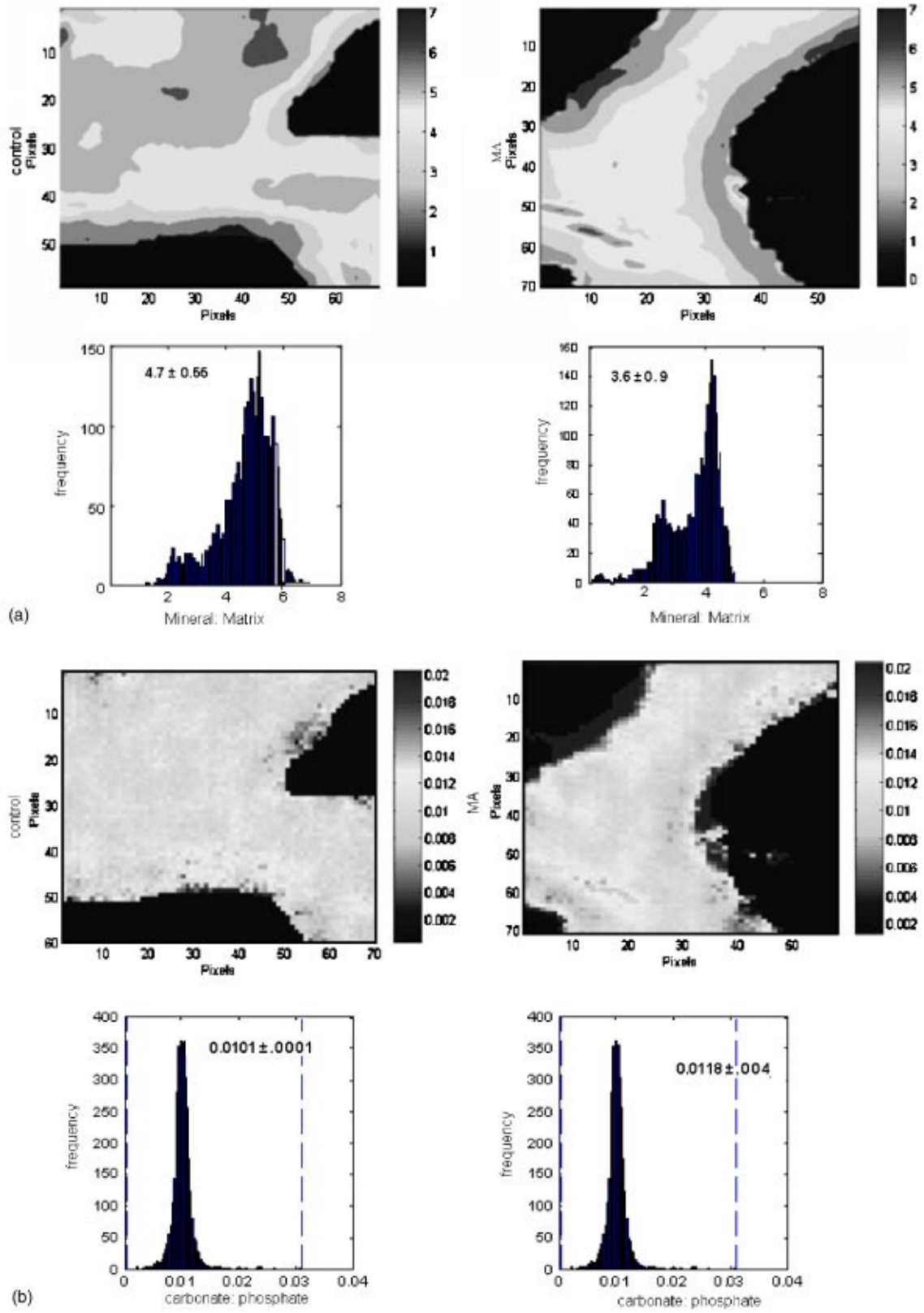

Fig. 7 Comparison of (a) the mineral: matrix ratio and (b) carbonate: phosphate ratio in vertebrae of a sheep with metabolic acidosis (left) contrasted with a normal age-matched control sheep (right). Pixel histograms show the distribution of parameters in the biopsy. Courtesy of Paul West, Hospital for Special Surgery.

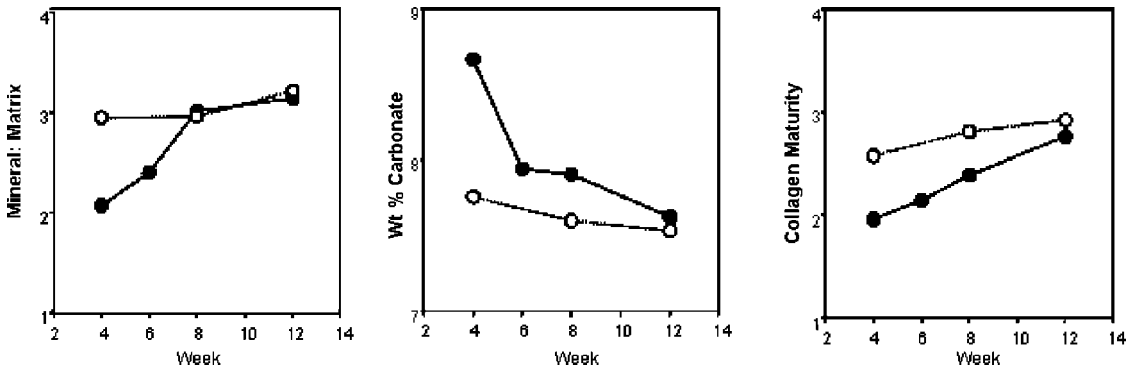

Fig. 8 Effect of estrogen (solid circles) on time-dependent changes in healing fracture callus in an ovariectomized rat is accelerated, and rapidly reaches the values seen in control bone (open circles) at a location distant from the fracture site in the same animals. Values are mean±S.D. for five rats. Courtesy of H. OuYang, thesis, Rutgers University, Department of Chemistry.

in trabecular bone of one normal and one untreated osteoporotic female. Typical of the osteoporotic cases studied to date, the trabeculae in the osteoporotic case are thinner than those in the normal; the mineral/matrix ratio in the osteoporotic patient is significantly reduced, while the bone crystallinity is increased. These all may contribute to the increased fragility of osteoporotic bone.

Comparable changes in IR parameters were found in ovariectomized monkeys[58–60] indicating the excellence of this model for studies of the human disease. Ovariectomized dogs failed to show the changes in mineral: matrix ratio and mineral crystallinity,[61] although they did manifest treatment-dependent changes. Similarly, in an unpublished pilot study of ovariectomized sheep ($n=5$) there were no significant changes in imaging parameters, however sheep subjected to metabolic acidosis (MA) did have changes in mineral to matrix ratio similar to those seen in osteoporotic humans [Fig. 7(a)]. The carbonate; phosphate distribution in the MA sheep was also different from that in the controls [Fig. 7(b)]. The pixel histograms describing the distributions of these parameters in the image shown are also presented.

Manipulation of genes in mice has become routine, and genetic polymorphisms associated with osteoporosis in humans can be examined in rodent models. While rodent models do not develop osteoporosis, they do lose bone, and hence, can be used for evaluating therapies, or validating spectroscopic parameters. Using congenic mice, Blank et al. was able to relate their mechanical strength to mineral: matrix ratio, and to show a direct correlation between this ratio and crystallinity.[62]

Overexpression of the vitamin D receptor in mice resulted in a phenotype in which calcium absorption was disturbed. There while bones were thicker and the distribution of peak calcium content as determined by backscatter electron imaging was increased and sharpened, there were, however, no changes in mineral content, mineral composition, crystallinity, particle size, or density as determined by a number of physicochemical techniques including IR.[63] Male and female mice in which the noncollagenous protein osteonectin expression is knocked out sustain rapid loss of trabeculae,[45] and IR microspectroscopy demonstrated an increase in collagen maturity, a decrease in mineral content, and an increase in crystal size, reminiscent of human changes in osteoporosis. Mice which lack osteocalcin expression, have thickened bones, and fail to resorb their bone. FTIR microspectroscopy demonstrated that the crystals were smaller although there were more crystals present, indicative of defective bone modeling in these animals.[64] Mice lacking the matrix protein, osteopontin, have increased mineral content, and unlike the osteocalcin deficient mice, increased crystal size,[65] implicating this protein both in regulation of crystal size and in regulation of remodeling. There are numerous other models which have been created to mimic human genetic defects associated with both decreased and increased bone density [e.g., Refs. 66–70], but their mineral properties, have not yet been reported.

3.3 *Therapies for Osteoporosis*

A large number of pharmaceutical interventions are currently being evaluated for the prevention and treatment of osteoporosis.[71] Because there are surrogate markers of bone quality, fewer and fewer biopsies are being collected for histomorphometric evaluation of bone turnover, thus there are fewer biopsies that can be used to quantify bone mineral properties. This has caused more and more reliance on the animal models discussed earlier. We have, however, shown that hormone replacement therapy in women just reaching their menopause improves bone quality,[72] Similarly, we have shown, in agreement with published data on mineral density,[73] that the selective estrogen receptor modulator, raloxifene, is not detrimental to bone quality (manuscript in preparation). Estrogen itself was demonstrated by IR imaging, as summarized in Fig. 8, to facilitate the rate of healing in a rat fracture injury model.[74]

Other studies reported determination of the effects of therapies on mineral quality in simian and rodent models. In a mouse model of brittle bone disease, a condition in man and mouse caused by a variety of mutations in the collagen gene, the bisphosphonate alendronate reduces fracture risk, without causing a statistically significant change in mineral crystallinity.[75,76] Similarly a study of dogs treated with both alendronate, and another bisphosphonate, risedronate, did not show significant changes in mineral properties as determined by IR of ground bones.[77] FTIR imaging of biopsies from osteoporotic patients or animal models treated with the bisphosphonates currently in clinical use are still needed.

Studies in monkeys have shown that parathyroid hormone increases new bone formation,[78] and that a bone resorption inhibitor, nandrolone decanoate, also improves bone quality by stimulating new bone formation, evidenced by increased acid phosphate, and carbonate content, and lower mineral: matrix ratios.[58] Ibandronate, another bisphosphonate,[79] and strontium ranelate,[80] drugs in clinical trial have been evaluated in monkeys, and the properties of those bones in the near future should be evaluated by IR methods.

4 Other Bone Diseases

In addition to osteoporosis, a great deal of information, beyond what could be acquired by standard histochemical techniques, is being learned from FTIR microspectroscopic studies of other bone diseases. In osteoarthritis, there is some debate as to whether the disease starts in bone and progresses to the overlying cartilage, or vice versa. FTIR analyses of human tissues[81] showed the mineral: matrix ratio was highest in normal cortical bone of the ulna, and lower in the sclerotic area of the affected site, which in turn was higher than values in loose bodies or trabecular bone of the tibia. This led the investigators to suggest that demineralization was considerably higher in osteoarthritis of the knee joint and remineralization was likely to occur under the acidic conditions in the articular region in this disease.

Osteogenesis imperfecta or brittle bone disease, as mentioned earlier, is a rare condition characterized by defects in the collagen gene and increased risk of fracture. FTIR analyses have demonstrated that the mineral: matrix ratio in the mouse model of a moderate-to-severe phenotype is reduced,[75] most likely because of a deficit in collagen content, and that the mineral crystals may be outside the collagen fibrils, and in general, are smaller than those in age-matched controls.[82] Other than a crystallographic evaluation of mineral crystal properties in humans with this disease,[82] and a recent Raman evaluation of a ''knock-in'' mutation,[83] there is little data on the effect of the various collagen mutations on mineral crystal size and perfection. Such analyses are extremely important as collagen provides the backbone on which bone mineral crystals deposit.

Osteopetrosis is another rare disease, this one due to abnormalities in the way osteoclasts (bone resorbing cells) develop. In this disease the marrow cavity is absent, and the bone is like rock because the remodeling process is impaired. Bone crystals in the rat model of this disease are decreased in size[84] while mineral content is increased. In a single human case, the same increase in mineral: matrix ratio and decrease in crystallinity was noted by infrared imaging.[85]

The last example is a more frequently observed disease, osteomalacia. This disease is caused by deficiencies in vitamin D. This vitamin is also the hormone that is responsible for regulating serum calcium levels, by regulating intestinal and kidney adsorption, and by contributing to the regulation of bone remodeling. In children, the disease is known as rickets, and is characterized by softened bones. In adults, the disease is manifest as an increased amount of unmineralized bone (osteoid). We used IR imaging to examine the mineralized matrix in patients with ''normal'' bone and patients diagnosed with osteomalacia. In the cortical bone, there were no differences in IR parameters when the unmineralized osteoid was excluded from analysis by spectral masking. In the trabecular bone, there was a general decrease in mineral content, a significant increase in matrix maturity, but no difference in crystallinity.[86] These differences could not be assessed by standard histomorphometry.

5 Conclusions

The application of infrared microspectroscopy and infrared microscopic imaging to the characterization of bone diseases and evaluation of the effects of therapies on the bone properties in these diseases is in its infancy. While IR has had a long history in the bone field, it is these newer applications that will have the greatest impact on the medical profession and on the population at large. The next generation of technological advances will include more sophisticated means for data processing, including cluster and factor analyses, and detectors for imaging instruments which will allow access to the υ_4 phosphate bands which currently cannot be examined with imaging spectrometers.

Acknowledgments

The studies carried out at the Hospital for Special Surgery and at Rutgers University as reported in this review were supported by NIH Grant No. AR041325 (A.L.B., P.I.) and from funds from the Busch Memorial fund of Rutgers University (to R.M.). The authors are deeply indebted to their students and collaborators, whose contributions over a 15 year period are detailed in the citations.

References

1. L. G. Raisz and G. A. Rodan, ''Pathogenesis of osteoporosis,'' *Endocrinol. Metab. Clin. North Am.* **32**, 15–24 (2003).
2. L. J. Melton III, C. S. Crowson, W. M. O'Fallon, H. W. Wahner, and B. L. Riggs, ''Relative contributions of bone density, bone turnover, and clinical risk factors to long-term fracture prediction,'' *J. Bone Miner. Res.* **18**, 312–318 (2003).
3. K. L. Stone, D. G. Seeley, L. Y. Lui, J. A. Cauley, K. Ensrud, W. S. Browner, M. C. Nevitt, and S. R. Cummings; Osteoporotic Fractures Research Group, ''BMD at multiple sites and risk of fracture of multiple types: long-term results from the study of osteoporotic fractures,'' *J. Bone Miner. Res.* **18**, 1947–1954 (2003).
4. G. I. Baroncelli, G. Federico, S. Bertelloni, F. Sodini, F. De Terlizzi, R. Cadossi, and G. Saggese, ''Assessment of bone quality by quantitative ultrasound of proximal phalanges of the hand and fracture rate in children and adolescents with bone and mineral disorders,'' *Pediatr. Res.* **54**, 125–136 (2004).
5. A. S. Posner and G. Duyckaerts, ''Infrared study of the carbonate in bone, teeth and francolite,'' *Experientia* **10**, 424–425 (1954).
6. A. S. Posner, ''Bone mineral on the molecular level,'' *Fed. Proc.* **32**, 1933–1937 (1973).
7. J. D. Termine and A. S. Posner, ''Infrared absorption of carbonate apatite,'' *Science* **155**, 607–608 (1967).
8. C. Rey, M. Shimizu, B. Collins, and M. J. Glimcher, ''Resolution-enhanced Fourier transform infrared spectroscopy study of the environment of phosphate ions in the early deposits of a solid phase of calcium-phosphate in bone and enamel, and their evolution with age. I:Investigations in the upsilon 4 PO4 domain,'' *Calcif. Tissue Int.* **46**, 384–394 (1990).
9. A. Bigi, E. Foresti, R. Gregorini, A. Ripamonti, N. Roveri, and J. S. Shah, ''The role of magnesium on the structure of biological apatites,'' *Calcif. Tissue Int.* **50**(5), 439–444 (1992).
10. M. D. Grynpas and C. Rey, ''The effect of fluoride treatment on bone mineral crystals in the rat,'' *Bone (N.Y.)* **13**, 423–429 (1992).
11. B. Turan, S. Bayari, C. Balcik, F. Severcan, and N. Akkas, ''A biomechanical and spectroscopic study of bone from rats with selenium deficiency and toxicity,'' *BioMetals* **13**, 113–121 (2000).
12. B. M. Kleber, D. Weigt, H. Weingart, E. Wachtel, L. A. Denisowa,

and L. S. Serowa, ''Structural changes in the dental hard substances and jaw bones of animals due to short-duration weightlessness,'' *Zahn Mund Kieferheilkd Zentralbl* **77**, 668–673 (1989).
13. H. Boyar, F. Zorlu, M. Mut, and F. Severcan, ''The effects of chronic hypoperfusion on rat cranial bone mineral and organic matrix. A Fourier transform infrared spectroscopy study,'' *Anal. Bioanal. Chem* **379**, 433–438 (2004).
14. J. D. Termine and A. S. Posner, ''Infrared analysis of rat bone: age dependency of amorphous and crystalline mineral fractions,'' *Science* **153**, 1523–1525 (1966).
15. A. Jikko, T. Aoba, H. Murakami, Y. Takano, M. Iwamoto, and Y. Kato, ''Characterization of the mineralization process in cultures of rabbit growth plate chondrocytes,'' *Dev. Biol.* **156**, 372–380 (1993).
16. S. Kale, S. Biermann, C. Edwards, C. Tarnowski, M. Morris, and M. W. Long, ''Three-dimensional cellular development is essential for *ex vivo* formation of human bone,'' *Nat. Biotechnol.* **18**, 954–958 (2000).
17. K. Satomura, K. Hiraiwa, and M. Nagayama, ''Mineralized nodule formation in rat bone marrow stromal cell culture without beta-glycerophosphate,'' *Bone Miner.* **14**, 41–54 (1991).
18. L. T. Kuhn, Y. Wu, C. Rey, L. C. Gerstenfeld, M. D. Grynpas, J. L. Ackerman, H. M. Kim, and M. J. Glimcher, ''Structure, composition, and maturation of newly deposited calcium-phosphate crystals in chicken osteoblast cell cultures,'' *J. Bone Miner. Res.* **15**, 1301–1309 (2000).
19. C. A. Luppen, N. Leclerc, T. Noh, A. Barski, A. Khokhar, A. L. Boskey, E. Smith, and B. Frenkel, ''Brief bone morphogenetic protein 2 treatment of glucocorticoid-inhibited MC3T3-E1 osteoblasts rescues commitment-associated cell cycle and mineralization without alteration of Runx2,'' *J. Biol. Chem.* **278**, 44995–45500 (2003).
20. L. F. Bonewald, S. E. Harris, J. Rosser, M. R. Dallas, S. L. Dallas, N. P. Camacho, B. Boyan, and A. Boskey, ''von Kossa staining alone is not sufficient to confirm that mineralization *in vitro* represents bone formation,'' *Calcif. Tissue Int.* **72**, 537–547 (2003).
21. Y. D. Halvorsen, D. Franklin, A. J. Bond, D. C. Hitt, C. Auchter, A. L. Boskey, E. P. Paschalis, W. O. Wilkison, and J. M. Gimble, ''Extracellular matrix mineralization and osteoblast gene expression by human adipose tissue-derived stromal cells,'' *Tissue Eng.* **7**, 729–741 (2001).
22. A. Oki, B. Parveen, S. Hossain, S. Adeniji, and H. Donahue, ''Preparation and in vitro bioactivity of zinc containing sol-gel-derived bioglass materials,'' *J. Biomed. Mater. Res.* **69A**, 216–221 (2004).
23. S. S. Liao and F. Z. Cui, ''*In vitro* and *in vivo* degradation of mineralized collagen-based composite scaffold: nanohydroxyapatite/collagen/poly(L-lactide),'' *Tissue Eng.* **10**, 73–80 (2004).
24. W. Xue, S. Tao, X. Liu, X. Zheng, and C. Ding, ''*In vivo* evaluation of plasma sprayed hydroxyapatite coatings having different crystallinity,'' *Biomaterials* **25**, 415–421 (2004).
25. J. Pinter, G. Lenart, and G. Rischak, ''Histologic, physical and chemical investigation of myositis ossificans traumatica,'' *Acta Orthop. Scand.* **51**, 899–902 (1980).
26. H. J. Tochon-Danguy, G. Boivin, M. Geoffroy, C. Walzer, and C. A. Baud, ''Physical and chemical analyses of the mineral substance during the development of two experimental cutaneous calcifications in rats: topical calciphylaxis and topical calcergy,'' *Z. Naturforsch [C]* **38**, 135–140 (1983).
27. C. Rey, J. Lian, M. Grynpas, F. Shapiro, L. Zylberberg, and M. J. Glimcher, ''Nonapatitic environments in bone mineral: FT-IR detection, biological properties and changes in several disease states,'' *Connect. Tissue Res.* **21**, 267–273 (1989).
28. J. Feinberg, O. Boachie-Adjei, P. G. Bullough, and A. L. Boskey, ''The distribution of calcific deposits in intervertebral discs of the lumbosacral spine,'' *Clin. Orthop. Relat. Res.* **254**, 303–310 (1990).
29. E. P. Paschalis, E. DiCarlo, F. Betts, P. Sherman, R. Mendelsohn, and A. L. Boskey, ''FTIR microspectroscopic analysis of human osteonal bone,'' *Calcif. Tissue Int.* **59**, 480–487 (1996).
30. R. Mendelsohn, A. Hassankhani, E. DiCarlo, and A. Boskey, ''FT-IR microscopy of endochondral ossification at 20 mu spatial resolution,'' *Calcif. Tissue Int.* **44**, 20–24 (1989).
31. C. Marcott, R. C. Reeder, E. P. Paschalis, D. N. Tatakis, A. L. Boskey, and R. Mendelsohn, ''Infrared microspectroscopic imaging of biomineralized tissues using a mercury-cadmium-telluride focal-plane array detector,'' *Cell Mol. Biol. (Paris)* **44**, 109–115 (1998).
32. A. L. Boskey, E. P. Paschalis, I. Binderman, and S. B. Doty, ''BMP-6 accelerates both chondrogenesis and mineral maturation in differentiating chick limb-bud mesenchymal cell cultures,'' *J. Cell. Biochem.* **84**, 509–519 (2002).
33. L. M. Childs, E. P. Paschalis, L. Xing, W. C. Dougall, D. Anderson, A. L. Boskey, J. E. Puzas, R. N. Rosier, R. J. O'Keefe, B. F. Boyce, and E. M. Schwarz, ''*In vivo* RANK signaling blockade using the receptor activator of NF-kappaB:Fc effectively prevents and ameliorates wear debris-induced osteolysis via osteoclast depletion without inhibiting osteogenesis,'' *J. Bone Miner. Res.* **17**, 192–199 (2002).
34. S. G. Kazarian, K. L. Chan, V. Maquet, and A. R. Boccaccini, ''Characterisation of bioactive and resorbable polylactide/Bioglass composites by FTIR spectroscopic imaging,'' *Biomaterials* **25**, 3931–3938 (2004).
35. J. Gokhale, P. G. Robey, and A. L. Boskey, ''The biochemistry of bone,'' in *Osteoporosis*, Robert Marcus, David Feldman, and Jennifer Kelsey, eds., 2nd ed., Vol. 1, pp. 107–189, Academic, San Diego (2001).
36. D. Pienkowski, T. M. Doers, M. C. Monier-Faugere, Z. Geng, N. P. Camacho, A. L. Boskey, and H. H. Malluche, ''Calcitonin alters bone quality in beagle dogs,'' *J. Bone Miner. Res.* **12**, 1936–1943 (1997).
37. C. Rey, V. Renugopalakrishnan, B. Collins, and M. J. Glimcher, ''Fourier transform infrared spectroscopic study of the carbonate ions in bone mineral during aging,'' *Calcif. Tissue Int.* **49**, 251–258 (1991).
38. N. Pleshko, A. Boskey, and R. Mendelsohn, ''Novel infrared spectroscopic method for the determination of crystallinity of hydroxyapatite minerals,'' *Biophys. J.* **60**, 786–793 (1991).
39. H. Ou-Yang, E. P. Paschalis, W. C. Mayo, A. L. Boskey, and R. Mendelsohn, ''Infrared microscopic imaging of bone: spatial distribution of CO3(2-),'' *J. Bone Miner. Res.* **16**, 893–900 (2001).
40. A. Aparicio, S. B. Doty, N. P. Camacho, E. P. Paschalis, L. Spevak, R. Mendelsohn, and A. L. Boskey, ''Optimal methods for processing mineralized tissues for Fourier transform infrared microspectroscopy,'' *Calcif. Tissue Int.* **70**, 422–429 (2002).
41. S. J. Gadaleta, E. P. Paschalis, F. Betts, R. Mendelsohn, and A. L. Boskey, ''Fourier transform infrared spectroscopy of the solution-mediated conversion of amorphous calcium phosphate to hydroxyapatite: new correlations between x-ray diffraction and infrared data,'' *Calcif. Tissue Int.* **58**, 9–16 (1996).
42. E. P. Paschalis, K. Verdelis, S. B. Doty, A. L. Boskey, R. Mendelsohn, and M. Yamauchi, ''Spectroscopic characterization of collagen cross-links in bone,'' *J. Bone Miner. Res.* **16**, 1821–1828 (2001).
43. L. M. Miller, V. Vairavamurthy, M. R. Chance, R. Mendelsohn, E. P. Paschalis, F. Betts, and A. L. Boskey, ''*In situ* analysis of mineral content and crystallinity in bone using infrared microspectroscopy of the $nu_4\,PO_4^{3-}$ vibration,'' *Biochim. Biophys. Acta* **1527**, 11–19 (2001).
44. H. Ou-Yang, E. P. Paschalis, A. L. Boskey, and R. Mendelsohn, ''Two-dimensional vibrational correlation spectroscopy of *in vitro* hydroxyapatite maturation,'' *Biopolymers* **57**, 129–139 (2000).
45. A. L. Boskey, D. J. Moore, M. Amling, E. Canalis, and A. M. Delany, ''Infrared analysis of the mineral and matrix in bones of osteonectin-null mice and their wildtype controls,'' *J. Bone Miner. Res.* **18**, 1005–1011 (2003).
46. A. L. Boskey, ''Bone mineral crystal size,'' *Osteoporosis Int.* **14**, 16–21 (2003).
47. C. H. Turner, L. P. Garetto, A. J. Dunipace, W. Zhang, M. E. Wilson, M. D. Grynpas, D. Chachra, D. R. McClintock, M. Peacock, and G. H. Stookey, ''Fluoride treatment increased serum IGF-1, bone turnover, and bone mass, but not bone strength, in rabbits,'' *Calcif. Tissue Int.* **61**, 77–83 (1997).
48. O. Akkus, F. Adar, and M. B. Schaffler, ''Age-related changes in physicochemical properties of mineral crystals are related to impaired mechanical function of cortical bone,'' *Bone (N.Y.)* **34**, 443–453 (2004).
49. M. C. van der Meulen, K. J. Jepsen, and B. Mikic, ''Understanding bone strength: size isn't everything,'' *Bone (N.Y.)* **29**, 101–104 (2001).
50. C. H. Turner, ''Biomechanics of bone: determinants of skeletal fragility and bone quality,'' *Osteoporosis Int.* **13**, 97–104 (2002).
51. L. Dalle, L. Carbonare, and S. Giannini, ''Bone microarchitecture as an important determinant of bone strength,'' *J. Endocrinol. Invest* **27**, 99–105 (2004).
52. S. H. Ralston, ''Genetic control of susceptibility to osteoporosis,'' *J. Clin. Endocrinol. Metab.* **87**, 2460–2466 (2002).
53. A. Bigi, G. Cojazzi, S. Panzavolta, A. Ripamonti, N. Roveri, M.

Romanello, K. Noris Suarez, and I. Moro, ''Chemical and structural characterization of the mineral phase from cortical and trabecular bone,'' *J. Inorg. Biochem.* **68**, 45–51 (1997).
54. L. Cohen and R. Kitzes, ''Infrared spectroscopy and magnesium content of bone mineral in osteoporotic women,'' *Isr J. Med. Sci.* **17**, 1123–1125 (1981).
55. D. D. Thompson, A. S. Posner, W. S. Laughlin, and N. C. Blumenthal, ''Comparison of bone apatite in osteoporotic and normal Eskimos,'' *Calcif. Tissue Int.* **35**, 392–393 (1983).
56. A. L. Boskey, ''Bone mineral and matrix. Are they altered in osteoporosis?,'' *Orthop. Clin. North Am.* **21**, 19–29 (1990).
57. E. P. Paschalis, F. Betts, E. DiCarlo, R. Mendelsohn, and A. L. Boskey, ''FTIR microspectroscopic analysis of human iliac crest biopsies from untreated osteoporotic bone,'' *Calcif. Tissue Int.* **61**, 487–492 (1997).
58. S. J. Gadeleta, A. L. Boskey, E. Paschalis, C. Carlson, F. Menschik, T. Baldini, M. Peterson, and C. M. Rimnac, ''A physical, chemical, and mechanical study of lumbar vertebrae from normal, ovariectomized, and nandrolone decanoate-treated cynomolgus monkeys (Macaca fascicularis),'' *Bone (N.Y.)* **27**, 541–550 (2000).
59. R. Y. Huang, L. M. Miller, C. S. Carlson, and M. R. Chance, ''Characterization of bone mineral composition in the proximal tibia of cynomolgus monkeys: effect of ovariectomy and nandrolone decanoate treatment,'' *Bone (N.Y.)* **30**, 492–497 (2002).
60. R. Y. Huang, L. M. Miller, C. S. Carlson, and M. R. Chance, ''*In situ* chemistry of osteoporosis revealed by synchrotron infrared microspectroscopy,'' *Bone (N.Y.)* **33**, 514–521 (2003).
61. M. C. Monier-Faugere, Z. Geng, E. P. Paschalis, Q. Qi, I. Arnala, F. Bauss, A. L. Boskey, and H. H. Malluche, ''Intermittent and continuous administration of the bisphosphonate ibandronate in ovariohysterectomized beagle dogs: effects on bone morphometry and mineral properties,'' *J. Bone Miner. Res.* **14**, 1768–1778 (1999).
62. R. D. Blank, T. H. Baldini, M. Kaufman, S. Bailey, R. Gupta, Y. Yershov, A. L. Boskey, S. N. Coppersmith, P. Demant, and E. P. Paschalis, ''Spectroscopically determined collagen Pyr/deH-DHLNL cross-link ratio and crystallinity indices differ markedly in recombinant congenic mice with divergent calculated bone tissue strength,'' *Connect. Tissue Res.* **44**, 134–142 (2003).
63. B. M. Misof, P. Roschger, W. Tesch, P. A. Baldock, A. Valenta, P. Messmer, J. A. Eisman, A. L. Boskey, E. M. Gardiner, P. Fratzl, and K. Klaushofer, ''Targeted overexpression of vitamin D receptor in osteoblasts increases calcium concentration without affecting structural properties of bone mineral crystals,'' *Calcif. Tissue Int.* **73**, 251–257 (2003).
64. A. L. Boskey, S. Gadaleta, C. Gundberg, S. B. Doty, P. Ducy, and G. Karsenty, ''Fourier transform infrared microspectroscopic analysis of bones of osteocalcin-deficient mice provides insight into the function of osteocalcin,'' *Bone (N.Y.)* **23**, 187–196 (1998).
65. A. L. Boskey, L. Spevak, E. Paschalis, S. B. Doty, and M. McKee, ''Osteopontin deficiency increases mineral content and mineral crystallinity in mouse bone,'' *Calcif. Tissue Int.* **71**, 145–154 (2002).
66. P. A. Baldock and I. A. Eisman, ''Genetic determinants of bone mass,'' *Curr. Opin. Rheumatol.* **16**, 450–456 (2004).
67. K. Iba, M. E. Durkin, L. Johnsen, E. Hunziker, K. Damgaard-Pedersen, H. Zhang, E. Engvall, R. Albrechtsen, and U. M. Wewer, ''Mice with a targeted deletion of the tetranectin gene exhibit a spinal deformity,'' *Mol. Cell. Biol.* **21**, 7817–7825 (2001).
68. Y. Murata, K. M. Robertson, M. E. Jones, and E. R. Simpson, ''Effect of estrogen deficiency in the male: the ArKO mouse model,'' *Mol. Cell Endocrinol.* **193**, 7–12 (2002).
69. L. K. McCauley, T. F. Tozum, K. M. Kozloff, A. J. Koh-Paige, C. Chen, M. Demashkieh, H. Cronovich, V. Richard, E. T. Keller, T. J. Rosol, and S. A. Goldstein, ''Transgenic models of metabolic bone disease: impact of estrogen receptor deficiency on skeletal metabolism,'' *Connect. Tissue Res.* **44**(1), 250–263 (2001).
70. P. Ducy, M. Amling, S. Takeda, M. Priemel, A. F. Schilling, F. T. Beil, J. Shen, C. Vinson, J. M. Rueger, and G. Karsenty, ''Leptin inhibits bone formation through a hypothalamic relay: a central control of bone mass,'' *Cell* **100**, 197–207 (2000).
71. B. R. MacDonald and M. Gowen, ''Emerging therapies in osteoporosis,'' *Best Pract. Res. Clin. Rheumatol.* **15**, 483–496 (2001).
72. E. P. Paschalis, A. L. Boskey, M. Kassem, and E. F. Eriksen, ''Effect of hormone replacement therapy on bone quality in early postmenopausal women,'' *J. Bone Miner. Res.* **18**, 955–959 (2003).
73. G. Boivin, P. Lips, S. M. Ott, K. D. Harper, S. Sarkar, K. V. Pinette, and P. J. Meunier, ''Contribution of raloxifene and calcium and vitamin D3 supplementation to the increase of the degree of mineralization of bone in postmenopausal women,'' *J. Clin. Endocrinol. Metab.* **884**, 199–205 (2003).
74. H. Ouyang, P. J. Sherman, E. P. Paschalis, A. L. Boskey, and R. Mendelsohn, ''Fourier transform infrared microscopic imaging: effects of estrogen and estrogen deficiency on fracture healing in rat femurs,'' *Appl. Spectrosc.* **58**, 1–9 (2004).
75. N. P. Camacho, W. J. Landis, and A. L. Boskey, ''Mineral changes in a mouse model of osteogenesis imperfecta detected by Fourier transform infrared microscopy,'' *Connect. Tissue Res.* **35**, 259–265 (1996).
76. N. P. Camacho, P. Carroll, and C. L. Raggio, ''Fourier transform infrared imaging spectroscopy (FT-IRIS) of mineralization in bisphosphonate-treated oim/oim mice,'' *Calcif. Tissue Int.* **72**, 604–609 (2003).
77. D. B. Burr, L. Miller, M. Grynpas, J. Li, A. Boyde, T. Mashiba, T. Hirano, and C. C. Johnston, ''Tissue mineralization is increased following 1-year treatment with high doses of bisphosphonates in dogs,'' *Bone (N.Y.)* **33**, 960–969 (2003).
78. E. P. Paschalis, D. B. Burr, R. Mendelsohn, J. M. Hock, and A. L. Boskey, ''Bone mineral and collagen quality in humeri of ovariectomized cynomolgus monkeys given rhPTH(1-34) for 18 months,'' *J. Bone Miner. Res.* **18**, 769–775 (2003).
79. F. Bauss and R. G. Russell, ''Ibandronate in osteoporosis: preclinical data and rationale for intermittent dosing,'' *Osteoporosis Int.* **15**, 423–433 (2004).
80. P. J. Marie, ''Optimizing bone metabolism in osteoporosis: insight into the pharmacologic profile of strontium ranelate,'' *Osteoporosis Int.* **14**, S9–S12 (2003).
81. M. Ueno, A. Shibata, S. Yasui, K. Yasuda, and K. Ohsaki, ''A proposal on the hard tissue remineralization in osteoarthritis of the knee joint investigated by FT-IR spectrometry,'' *Cell Mol. Biol. (Paris)* **49**, 613–619 (2003).
82. U. Vetter, E. D. Eanes, J. B. Kopp, J. D. Termine, and P. G. Robey, ''Changes in apatite crystal size in bones of patients with osteogenesis imperfecta,'' *Calcif. Tissue Int.* **49**, 248–250 (1991).
83. K. M. Kozloff, A. Carden, C. Bergwitz, A. Forlino, T. E. Uveges, M. D. Morris, J. C. Marini, and S. A. Goldstein, ''Brittle IV mouse model for osteogenesis imperfecta IV demonstrates postpubertal adaptations to improve whole bone strength,'' *J. Bone Miner. Res.* **19**, 614–622 (2004).
84. A. L. Boskey and S. C. Marks, Jr., ''Mineral and matrix alterations in the bones of incisors-absent (ia/ia) osteopetrotic rats,'' *Calcif. Tissue Int.* **37**, 287–292 (1985).
85. A. Boskey, ''Mineral changes in osteopetrosis,'' *Crit. Rev. Eukaryot Gene Expr* **13**, 109–116 (2003).
86. D. Faibish, A. Gomez, G. Boivin, I. Binderman, and A. L. Boskey, ''Infrared imaging of calcified tissues in bone biopsies from adults with osteomalacia'' *Bone* **36**, 6–12 (2005).